TIME EVOLUTION AND INTER-ANNUAL VARIABILITY OF SEASONAL ICE ON THE MARS NORTHERN POLAR CAP. C. Mount[1,2] and T. N. Titus[2], [1]Northern Arizona University, Flagstaff, AZ 86001 (cmount@usgs.gov), [2]U.S.G.S., 2255 N. Gemini Dr., Flagstaff, AZ 86001 (ttitus@usgs.gov).

Introduction: The seasonal polar caps are among the most active regions on Mars. Approximately twenty-five percent of Mars' total atmosphere cycles annually through the seasonal polar caps [1,2], significantly influencing global climate variations. There are thought to be two primary forms of CO_2 ice deposition on Mars: 1) direct formation of ice onto the surface (slab CO_2) and 2) CO_2 condensing in the atmosphere and precipitating onto the surface (i.e., CO_2 snow) [3,4]. Time-dependent density variations in these ices may indicate which of these processes was responsible for the deposition. We expect densities of CO_2 snow-like deposits to increase throughout the sublimation cycle due to compaction and settling [5], whereas the more cohesive CO_2 slab ice deposits would maintain relatively constant densities before starting to fracture near the end of the sublimation cycle.

Here we explore the temporal density variations of Mars' Northern Polar Seasonal Ice Cap (NPSC), and discuss the processes responsible for seasonal ice deposition. We also use ice depth and density estimates to constrain the date of Complete Recession of CO_2 Under Sublimation (CROCUS) [6] for a specific location and compare it to the CROCUS dates from three previous Mars years.

Data: The findings presented here focus on a section of the NPSC between latitudes 65°N and 75°N. Preliminary data were analyzed for one location: inside a crater located at 70.1°N, 103.4°E.

We utilize High Resolution Imaging Science Experiment (HiRISE) data from Mars Years (MY) 28-29 and Thermal Emission Spectrometer (TES) data from MY 24-26 [7]. Note that HiRISE and TES data are taken from different years due to lack of mission overlap, so inter-annual variations will introduce some uncertainties into the volume density estimates.

Technique: Volume density may be calculated by dividing the column abundance of CO_2 by the depth of the ice cap in a region. Column abundances are derived in a variety of ways: energy balance calculations [2,6,8], neutron [5,9,10], gamma ray [1,10] spectroscopy and variations in the gravity field [11,12,13]. Most density studies of the Martian Polar Caps use the Mars Orbiter Laser Altimeter (MOLA) to measure the depth of the cap [5,9,11,12,13], although the seasonal changes in rock heights on the surface can be used to measure ice depths to a greater accuracy [4].

A region is comprised of a set of HiRISE images spanning a significant seasonal range and including a corresponding summer image. Each region is subdivided into sub-regions. Sub-regional measurements are averaged together to give regional averages for the ice depth and column abundance.

Measurements for the ice depth are determined using the method from [4] in which rock shadow lengths are measured in HiRISE images, though we do not assume the rocks are on flat ground (slope = 0°). Slopes were calculated using elevation data from MOLA. We approximate all the rocks in a sub-region to lie on a plane with its gradient in the direction of the incident ray at that areocentric longitude (L_s). From a geometric relationship between the shadow length, the angle of the incident ray, and the slope, the rock height can be found. The heights of the rocks in spring images are then compared to those in a late summer image known to have no ice. The average difference in the heights of the rocks yields the seasonal ice depth.

Column abundances were derived from TES albedo and bolometric temperature observations combined with the sublimation and energy balance techniques as described in [6] and [7].

Results: Preliminary data for the regionally averaged ice depth between L_s ~12° and 48° is presented below in Figure 1. Surprisingly, the ice depth increases from L_s ~12° to 17°. We attribute this increase to condensation occurring on the tops of the rocks measured in early spring. When the ice sublimes from the tops of the rocks, it gives the illusion that the ice depth is increasing, when in actuality the measured rock height is decreasing. This means the initial depth may be much greater than that presented.

The depth of the ice decreases to negative at L_s ~38°. This negative depth could be attributed to some systematic or random error, such as changes in shadow length due to non-uniform topography, changes in the illumination azimuth, ice buildup on the tops of the rocks, or the melting of ice around rocks causing "moating" due to high thermal inertia [12]. We interpret negative depths as zero. This allows us to constrain the regional CROCUS date in MY 29 to be as early as L_s ~33°.

Figure 2 shows the column abundance for MY 24-26; it is highly dependent on the CROCUS date. The column abundance has the same general trend on a yearly basis, but the TES observed CROCUS dates vary markedly (see Table 1). This constrains the CROCUS date in MY 29 to be as late as L_s ~42°.

The average initial density is presented in Table 2. This is important because the early spring density will be most indicative of what type of ice (slab or snow) is

observed. Since the depth measured at L_s ~12° is suspect, the density at L_s ~17° is most indicative of the depositional mechanism. The average initial densities are consistent with CO_2 snow, indicating precipitation as the depositional mechanism in this region. The time-averaged densities (Table 2) are consistent with numerous 'global,' time-averaged density studies of the NPSC [1,5,11,14]. The ice becomes less dense throughout the sublimation season, although the errors on the density are significantly large such that the ice density may remain constant. This is contrary to the findings of [13], who found seasonal CO_2 snow-like deposits densified throughout sublimation. However, their analysis was for 'globally' averaged densities, whereas this study focuses on the density of localized regions. Time evolution of the ice density may be found in Figure 3.

Averaging the constraints from all years, we find the CROCUS date in MY 29 to be slightly earlier than other years as observed by TES (see Table 1).

MY	24	25	26	29
CROCUS	38.8	41.8	40.8	36.7±3.8

Table 1. Regional CROCUS date for each Mars Year. The CROCUS date for MY 29 is earlier than MY 24-26 (TES).

MY	24		25		26	
Average Initial	540	+94 -215	666	+116 +248	587	+102 -231
Time-averaged	432	+102 -205	581	+146 -258	500	+123 -233

Table 2. Initial and time-averaged densities for MY 24-26. The plus and minus values are the upper and lower uncertainties, respectively.

Conclusion: Preliminary results taken for one location on the NPSC are consistent with the findings of numerous 'global,' time-averaged, ice density studies [1,5,11,14]. The initial density suggests CO_2 precipitation as the primary deposition mechanism for this location. The site exhibits de-densification throughout sublimation though error analysis indicates the ice density could be static.

Through ice depth and ice density estimates, we were able to constrain the CROCUS date in MY 29. The CROCUS date is earlier than those observed by TES, suggesting perhaps MY 29 was an earlier year for CROCUS on the NPSC than other Mars Years.

More locations must to be studied to analyze the spatial variability of these results.

References: [1] Kelly, N. J. et al. (2006), *JGR*, *111*, E03S07 [printed *112*(E3), 2007]. [2] Titus, T. N. et al. (2008), in *The Martian Surf.: Comp., Mineralogy, and Phys. Prop.*, Edited by J. F. Bell III, Cambridge University Press., 578-598. [3] Titus, T. N. et al. (2001), *JGR*, *106*, 23181-23196. [4] Cull, S. et al. (2010), *JGR*, *115*, E00D16. [5] Aharonson, O. et al. (2004), *JGR*, *109*, E05004. [6] Kieffer, H. H. et al. (2000), *JGR*, *104*, 9653-9699. [7] Clancy, R. T. et al. (2000), *JGR*, *105*(E4), 9553-9571. [8] Kieffer, H. H. and Titus, T. N. (2001), *Icarus*, *154*, 162-180. [9] Prettyman et al. (2009), *JGR*, *114*, E08005. [10] Feldman, W. C. et al. (2003), *JGR*, *108*(E9), 5103. [11] Smith, D. E. et al. (2001), *Science*, *294*, 2141-2146. [12] Smith, D. E. et al. (2009), *JGR*, *114*, E05002. [13] Matsuo, K. and Heki, K. (2009), *Icarus*, *202*, 90-94. [14] Haberle R. M. et al. (2004), *GRL*, *31*, L057025.

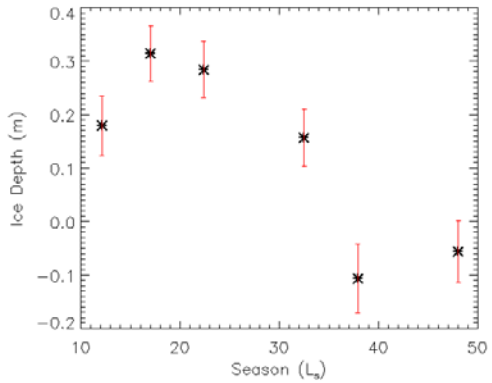

Figure 1. Regionally averaged ice depth vs. season. The depth is negative at L_s ~38°, constraining the CROCUS date to be as early as L_s ~33°. Note the depth at L_s ~12° could be larger due to ice condensation on the tops of rocks in early spring.

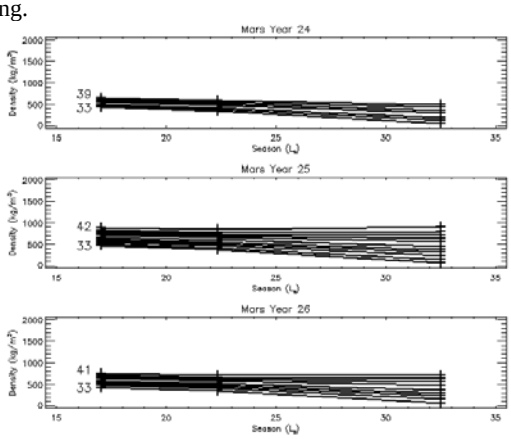

Figure 2. Column abundance vs. season for MY 24-26; it is highly dependent on the CROCUS date. The numbers on the left indicate the approximate CROCUS date for the upper most and lower most curves, with each curve separated by 1° of L_s in CROCUS date.

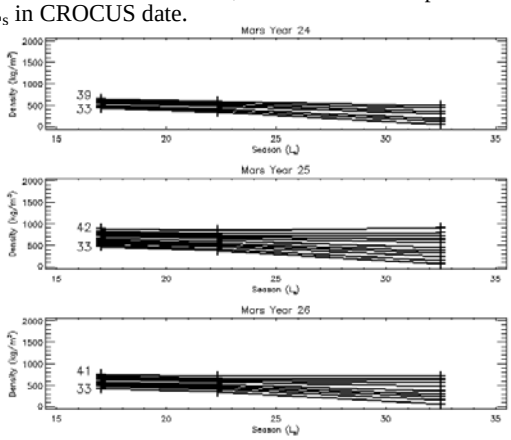

Figure 3. Density vs. season using column abundances from MY 24-26 and ice depths as determined in MY 29. The numbers on the left indicate the approximate CROCUS date for the upper most and lower most curves, with each curve separated by 1° of L_s in CROCUS date.